Structure, Vol. 13, 861–871, June, 2005, ©2005 Elsevier Ltd All rights reserved. DOI 10.1016/j.str.2005.03.012

The Crystal Structure of a c-Src Complex in an Active Conformation Suggests Possible Steps in c-Src Activation

Sandra W. Cowan-Jacob,[1,*] Gabriele Fendrich,[1] Paul W. Manley,[2] Wolfgang Jahnke,[1] Doriano Fabbro,[2] Janis Liebetanz,[2] and Thomas Meyer[2]
[1]Discovery Technologies
[2]Oncology Research Department
Novartis Institutes for Biomedical Research
CH-4056 Basel
Switzerland

Summary

The regulation of the activity of Abl and Src family tyrosine kinases is mediated by intramolecular interactions between the SH3, SH2, and kinase (SH1) domains. We have determined the crystal structure of an unphosphorylated form of c-Src in which the SH2 domain is not bound to the C-terminal tail. This results in an open structure where the kinase domain adopts an active conformation and the C terminus binds within a hydrophobic pocket in the C-terminal lobe. NMR binding studies support the hypothesis that an N-terminal myristate could bind in this pocket, as observed for Abl, suggesting that c-Src may also be regulated by myristate binding. In addition, the structure contains a des-methyl analog of the antileukemia drug imatinib (STI571; Gleevec). This structure reveals why the drug shows a low affinity for active kinase conformations, contributing to its excellent kinase selectivity profile.

Introduction

The BCR-ABL gene is the cause of chronic myelogenous leukemia (CML), and some acute lymphoblastic leukemias (ALL) (Sawyers, 1999). This oncogene encodes the Bcr-Abl protein, which possesses a constitutively activated Abl tyrosine kinase domain that abrogates the growth factor requirements for the proliferation and survival of hematopoietic cells by unregulated phosphorylation of cellular proteins (Deininger et al., 2000; Faderl et al., 1999; Sawyers, 1999). The antileukemia drug, imatinib, acts by selectively inhibiting the tyrosine kinase activity of Bcr-Abl (Capdeville et al., 2002). Although clinical responses to STI571 in patients with stable-phase CML are durable (Hughes et al., 2003), patients in late-stage disease frequently develop drug resistance and relapse (Kantarjian et al., 2002). Relapse is often associated with point mutations in the Bcr-Abl kinase domain that reduce the affinity of imatinib (Gorre et al., 2001; Cowan-Jacob et al., 2004; Hochhaus and La Rosee, 2004). A possible approach to circumventing patient relapse is to inhibit downstream signaling stimulated by Bcr-Abl phosphorylation or block alternative signaling pathways that lead to Ph^+ cell survival. Inhibition of c-Src kinase activity could provide a combined strategy for these approaches, as Bcr-Abl has been shown to activate c-Src by phosphorylation and the growth factor interleukin-3, which signals through the c-Src pathway, has been shown to rescue Bcr-Abl-expressing cells in the presence of antiproliferative concentrations of STI571 (Warmuth et al., 2003).

Members of the c-Src-family of kinases all contain SH3, SH2, and kinase (SH1) domains followed by a short C-terminal regulation segment. Phosphorylation of Tyr527 in the C-terminal tail is found to downregulate the kinase activity, and phosphorylation of Tyr416 in the activation loop is necessary for full kinase activity. One or the other of the tyrosines in the cellular enzyme is phosphorylated, but not both. Structures of both human and chicken c-Src (Williams et al., 1997; Xu et al., 1997, 1999) phosphorylated on Tyr527 (chicken c-Src numbering) revealed an autoinhibitory state of the protein, referred to as the "assembled regulatory domain" conformation. There are several components of this assembly that negatively regulate the activity of the kinase domain. The position of helix αC, the conformation of the activation loop, and the configuration of the remaining catalytic machinery, all in the kinase domain, make a direct contribution because they are unsuitable for activity. The binding of the SH3 domain to the linker between the SH2 and kinase domains, and the binding of the SH2 domain to p-Tyr527 on the C-terminal tail, will inhibit the interaction of these domains with other cellular proteins that have been shown to enhance the activity of c-Src and may restrain the protein from adopting a fully active conformation, but they will not necessarily prevent some residual activity (Lerner and Smithgall, 2002).

Although the N-terminal region of c-Abl contains a similar arrangement of SH3, SH2, and kinase domains that have a role in the regulation of the kinase activity, it lacks a phosphorylation site equivalent to Tyr527 in the c-Src family of tyrosine kinases. Recent structural and functional studies (Pluk et al., 2002; Nagar et al., 2003; Hantschel et al., 2003), have shown that at least the 1a form of Abl contains an N-terminal myristyl modification, which is able to bind in a pocket located in the C-terminal lobe of the kinase domain, thus locking the protein into an autoinhibitory assembled conformation very similar to that of the c-Src and Hck structures (Sicheri et al., 1997; Williams et al., 1997; Schindler et al., 1999; Xu et al., 1997, 1999). The inactive conformation of the c-Src family kinase domains and that of c-Abl are, however, significantly different (Schindler et al., 2000; Nagar et al., 2003). This helps to explain why STI571 binds strongly to c-Abl, but only very weakly to c-Src, because it is known that STI571 has high affinity for the specific inactive conformation of c-Abl, but very low affinity for the active conformation of the kinase (Schindler et al., 2000).

During the optimization of the Bcr-Abl kinase inhibitory activity of STI571, the activity of the lead compound 1 against c-Src was removed by incorporating a methyl group (Figure 1). Reintroducing this activity into the STI571 structure might therefore lead to com-

*Correspondence: sandra.jacob@novartis.com

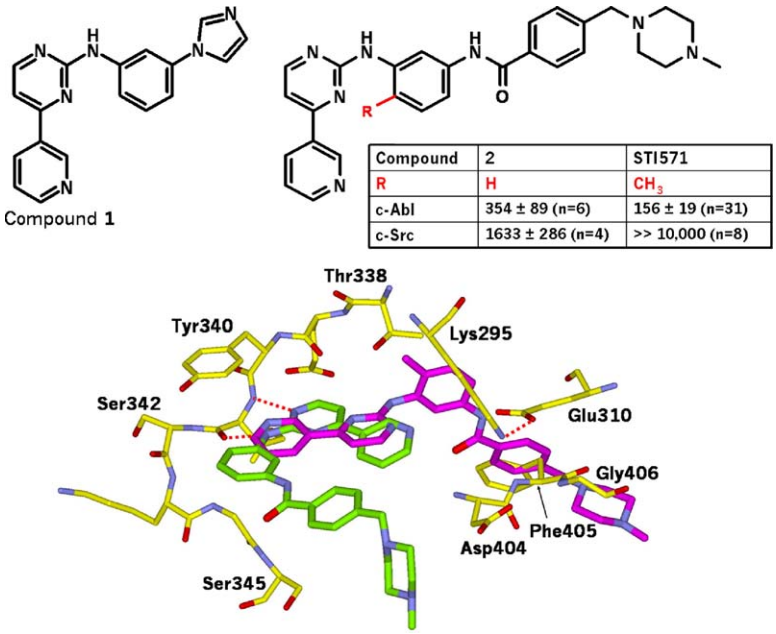

Figure 1. Chemical Structures Referred to in this Article and Details of the Binding of Compound **2** to c-Src

(Top) The IC_{50} values for inhibition of trans-phosphorylation by compound **2** and STI571 versus c-Src and Abl kinase are shown in nanomolar concentrations (description of measurements provided as Supplemental Data).

(Bottom) Details of the binding of compound **2** (green) to c-Src (yellow) showing hydrogen bonds with red dashed lines. The structure of STI571 (magenta) as bound to Abl kinase is superimposed.

pounds that could be capable of circumventing STI571 resistance in CML patients. Combined Abl-Src inhibitors have recently been described, and BMS-354825 has entered phase II clinical trials (O'hare et al., 2004; Shah et al., 2004). In order to understand the structural basis of why STI571 did not inhibit c-Src, we carried out structural biology studies with an analog of STI571, **2**, which retained activity against c-Src. In addition to revealing why STI571 does not strongly inhibit the kinase activity of c-Src, the X-ray crystal structure of the complex between **2** and c-Src has revealed a new, partially assembled state of the protein in which the kinase domain adopts an active conformation.

Results

Protein Preparation

Human c-Src tyrosine kinase is a multidomain protein of 535 amino acids (Boggon and Eck, 2004). The full-length protein exhibits limited solubility and stability, making it unsuitable for structural studies. Mutants of c-Src lacking the N-terminal myristylation site and the "unique" domain, but including SH3, SH2, kinase domain and C-terminal tail, have been described (Ellis, 1994) and a construct with the N-terminal amino acids Gly1–Gly84 (human numbering) deleted has been successfully crystallized (Xu et al., 1997) when phosphorylated at Tyr529 (Tyr527, chicken numbering) of the C-terminal tail. The amino acid numbering of chicken c-Src will be used subsequently here for consistency with earlier publications.

Expression of this c-Src construct in Sf9 cells led to a mixture of un-, mono-, and diphosphorylated forms, the unphosphorylated form representing about one third of the total c-Src. Addition of a c-Src inhibitor to the cell culture at the time of viral infection increased the fraction of the unphosphorylated form to ~70%; the remainder of the expressed c-Src was monophosphorylated. The two forms could be separated by conventional ion-exchange chromatography, which also removed the inhibitor and allowed subsequent recomplexation of the purified unphosphorylated c-Src with compound **2**.

Structure Determination of Unphosphorylated c-Src

Diffraction data were collected for a single crystal of c-Src in complex with compound **2**, which grew to 0.25 × 0.25 × 0.25 mm^3 in size in 1.3 M $(NH_4)_2SO_4$, 0.1 M Tris (pH 8.0) and 12% glycerol (Table 1). The structure was solved using single domains of the assembled structure (PDB entry 2SRC) as individual search models in molecular replacement and refined using all data between 40.0 and 1.9 Å resolution (Table 1). Electron density for compound **2** was clearly visible from the early stages of refinement, although only the pyridinyl, pyrimidinyl, and diaminophenyl rings of the inhibitor are well defined (see Figure S1 in the Supplemental Data available with this article online). Weak residual density for the remainder of the inhibitor was fitted in the latter stages of refinement; however, the occupancy of this part of the inhibitor is low, reflecting the fact that it is flexible and probably adopts multiple conformations in the crystal. The final model consists of residues 83–533 (chicken numbering) of c-Src plus an N-terminal methionine (82), compound **2**, five sulfate ions that originate from the crystallization buffer, and 315 water molecules. The coordinates and structure factors have been deposited in the protein data bank with PDB entries 1Y57 and 1Y57SF.

The Overall Structure of Unphosphorylated c-Src

The structures of the SH3, SH2, and kinase domains of unphosphorylated c-Src resemble the published struc-

Table 1. Crystallographic Data Collection and Refinement Statistics

Data Collection		Refinement	
Space group	$P4_12_12$	R factor	0.188
Unit Cell dimensions (Å)	a = b = 106.21; c = 123.73	R free	0.213
Solvent content (%)	64 (V_M = 3.38 Å^3/Da)	Free R test size (no., %)	2813, 5.1
Molecules in the asymmetric unit (no.)	1	Protein residues and atoms (no.)	452, 3600
Resolution range (Å) (last shell)	40.0–1.90 (1.97–1.90)	Heterogen atoms (no.)	36
Measured reflections (no.)	393,745	Solvent atoms (no.)	315
Unique reflections (no.)	55,642	Sulfate groups (no.)	5
Redundancy	7.1	Rmsd bond lengths (Å)	0.011
Completeness (%)	99.8 (99.6)[a]	Rmsd bond angles (°)	1.25
R_{sym} (%)[b]	9.0 (43.5)[a]	Average B factors (Å^2) (overall, protein, inhibitor, water, sulfate)	27.52, 30.09, 45.59, 45.14, 65.75
% reflections with I/Sig(I) > 2	80.2 (43.1)[a]		

[a] Values presented are overall resolution, with values in parentheses being from highest resolution shell.
[b] $R_{sym} = \Sigma \mid I - \langle I \rangle \mid / \Sigma I$, where I is the observed intensity of a reflection and <I> is the average intensity of multiple observations of symmetry-related reflections.

tures of the individual domains (Waksman et al., 1992; Feng et al., 1994) and those of the assembled inactive state (Xu et al., 1997, 1999). However, the lack of phosphorylation of Tyr527 means that the SH2 domain is not locked down beside the C-terminal lobe of the kinase domain in the crystals. The SH3 and SH2 domains are found to lie approximately at right angles to the kinase domain with only the SH3 domain and linker in contact with the N-terminal lobe, where they stack alongside helix αC (Figure 2). The SH3 domain is bound to the linker between the SH2 domain and the kinase domain, as observed in the assembled inactive conformation (Xu et al., 1999). The SH2 domain binding site contains sulfate ions from the crystallization buffer and water molecules. The unphosphorylated C-terminal tail is well defined in the electron density and folds back into the C-terminal lobe of the kinase domain, where it becomes an integral part of the structure. In fact, the C-terminal leucine is found to bind in a pocket that is used by myristate in the assembled inactive conformation of c-Abl (Nagar et al., 2003) (Figure 3). The kinase domain itself has undergone significant conformational changes, and helix αC now occupies the position that is observed for active kinases. The activation loop does not block the active site and has an extended conformation that also resembles an active kinase, although phosphorylation of Tyr416 would be required for the loop to form a suitable platform for the binding of substrate. The N- and C-terminal lobes of the kinase have rotated away from each other by approximately 13° (through an axis passing close to the Cα positions of Lys343 in the hinge, Met314 in αC, and Val323 of the

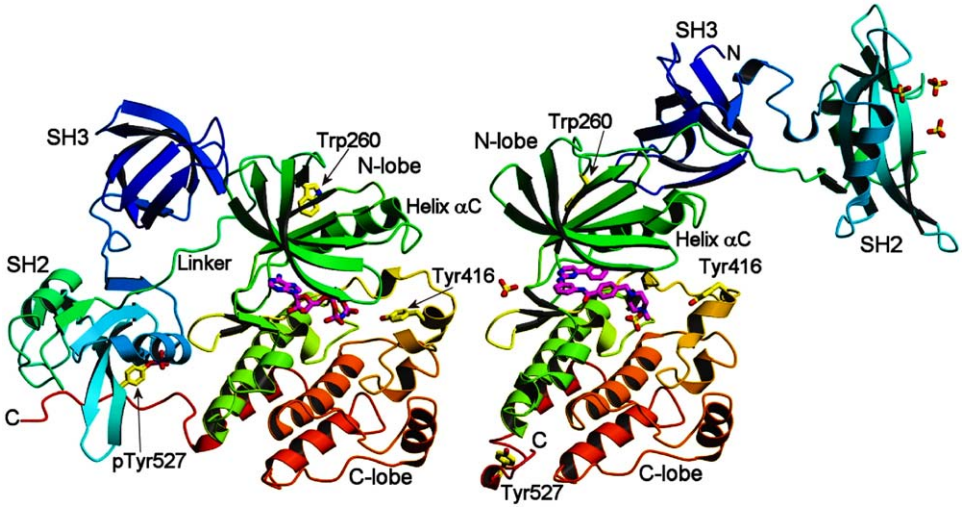

Figure 2. Conformational States of c-Src

Comparison of the structures of human c-Src phosphorylated on Tyr527 (left) and in the unphosphorylated state (right). Both structures have the same orientation with respect to their C-terminal lobes, which were superimposed. The ribbon diagrams are colored from dark blue at the N terminus to red at the C terminus; thus, the SH3 domain is blue, the SH2 domain is light blue and green, the linker is aqua, the N-terminal lobe is green, the C-terminal lobe is light green and orange, the activation loop is yellow, and the C-terminal tail is red. The ligands (magenta), sulfate groups (yellow and red), and certain side chains (yellow) discussed in the text are also represented.

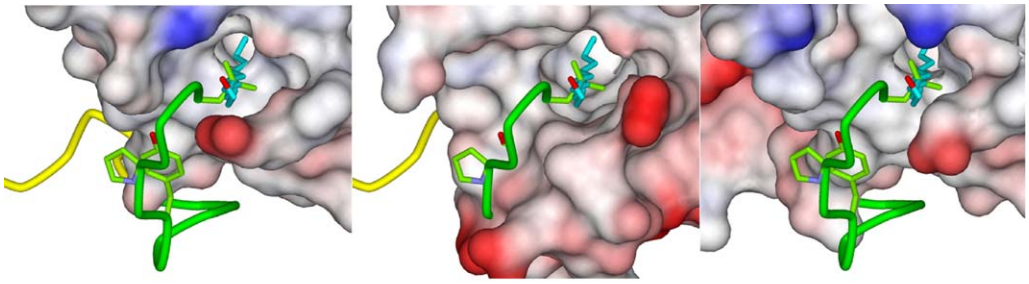

```
HCK       LPKLIDFS...LMEIVTY...ENCPEELYN-IMMRCWKNRPEERPTFEYIQSVLDDFYTATESQYQQQP------
LYN       LPKLIDFS...LYEIVTY...ENCPDELYD-IMKMCWKEKAEERPTFDYLQSVLDDFYTATEGQYQQQP------
LCK       INKLLDMA...LTEIVTH...DNCPEELYQ-LMRLCWKERPEDRPTFDYLRSVLEDFFTATEGQYQPQP------
BLK       LPRLIDMS...LMEVVTY...DTCPPELYRGVIAECWRSRPEERPTFEFLQSVLEDFYTATERQYELQP------
        360        452       485                                    #     533
SRC       LPQLVDMA...LTELTTK...PECPESLHD-LMCQCWRKEPEERPTFEYLQAFLEDYFTSTEPQYQPGENL----
YES       LPQLVDMA...LTELVTK...QGCPESLHE-LMNLCWKKDPDERPTFEYIQSFLEDYFTATEPQYQPGENL----
YRK       LPQLVDMA...LTELVTK...GGCPPSLHD-VMVQCWKREPEERPTFEYLQSFLEDYFTATEPQYQPGDNQ----
FYN       LPNLVDMA...LTELVTK...QDCPISLHE-LMIHCWKKDPEERPTFEYLQSFLEDYFTATEPQYQPGENL----
FGR       LPQLVDMA...LTELITK...PGCPASLYE-AMEQTWRLDPEERPTFEYLQSFLEDYFTSAEPQYQPGDQT----
          M  MM  B   B   M E    M M  M  -B                    B
ABL       AVVLLYMA...LWEIATY...EGCPEKVYE-LMRACWQWNPSDRPSFAEIHQAFETMFQESSISDEVEKELGKQG
          :  *: ::   * *: *      **  ::   :   *:  . :**:*  ::  ::  :
```

Figure 3. The Potential Myristate Binding Pocket

(Top) Superposition of the unphosphorylated c-Src structure (green) with the structure of the myristate bound c-Abl (PDB accession code 1OPJ, cyan), showing the path of the phosphorylated C-terminal tail of pTyr527 c-Src in yellow. Solvent-accessible surfaces are superimposed for: unphosphorylated c-Src calculated excluding the C-terminal tail (left), Abl kinase (middle), and pTyr527 c-Src (right). The Tyr527 side chain of unphosphorylated c-Src is shielded by Pro529, and Leu533 binds in the upper half of the pocket with respect to myristate.

(Bottom) Sequence alignment comparing the C-terminal regions of the Src-family kinases and that of Abl, plus other residues lining the potential myristate binding pocket (E, entrance; M, middle; B, bottom of pocket; #, tyr527; *, strictly conserved; :, conservative substitutions).

αC-β4 loop), leaving more space in the cleft between them, which is required for the binding of compound **2**.

Inhibitor Binding

Compound **2** binds in the adenine binding site of ATP, making two hydrogen bonds to Met341 of the hinge region between the two lobes in a similar fashion to that of many kinase inhibitors (Figure 1). The pyridinyl, pyrimidine, and diaminophenyl groups are well defined in the electron density, although the exact orientation of the pyridinyl ring can not be defined due to the lack of hydrogen bonds that would indicate the position of the nitrogen atom. The rest of the inhibitor lies close to the ribose binding site of ATP, but is largely exposed to solvent. The three rings in the adenine binding site are coplanar. Other residues lining the binding site include: Leu273, Gly274, Gln275, and Val281 from the glycine-rich or P loop, Ala293 from β3 of the N-terminal lobe, Glu339 and Tyr340 from the hinge region, and Leu393 from the N-terminal part of the activation loop.

This mode of binding is clearly different from that observed for STI571 to c-Abl (Figure 1). The presence of the 6-methyl group on the diaminophenyl ring means that a noncoplanar conformation of the diarylamine moiety is preferred in STI571. This is the conformation that is required for STI571 to bind to the inactive conformation of c-Abl (Schindler et al., 2000). Assuming that c-Src cannot adopt the same inactive conformation as observed for c-Abl (Nagar et al., 2002), despite the high sequence identity between the two kinases, in order for STI571 to bind to c-Src it would have to adopt a coplanar arrangement of the pyridinyl, pyrimidinyl, and diaminophenyl rings, and furthermore, the presence of the methyl group would weaken the hydrogen bonds to the hinge region of c-Src due to steric clashes with main chain atoms of Met341 and Ser342. This has recently been observed for STI571 in complex with Syk kinase (Atwell et al., 2004).

SH2 and SH3 Domain Structure

The SH3 and SH2 domains are rotated by about 130° compared to their position in the assembled inactive state; however, they have retained the "clamp" structure (Harrison, 2003), in which the SH3 domain remains bound to the linker. Although the individual structures of the domains have changed very little (rmsd values of 1.1 and 0.7 Å for the SH3 and SH2 domains, respectively), the relative angle between the two domains has increased by about 25°, resulting in a shift of up to 12 Å for residues of the SH2 domain when the SH3 domains are superimposed (Figure 4). The hinge region for this motion lies between the SH3 and SH2 domains, near Ser140, and also involves residues from the linker around Thr247. This flexibility has previously been recognized by comparing solution (NMR) and crystal structures of SH3-SH2 domains from proteins such as Fyn, Lck, Abl, and c-Src (Ulmer et al., 2002) compared to all the other structures and the open conformation observed here. The conformation adopted in the assembled inactive state of c-Src is closed. The actual structure of the residues in the hinge region has changed very little (Figure 4), except that Ser140 undergoes a peptide plane flip of 180°, and, along with Asp141, it makes hydrogen bonds to the main chain of

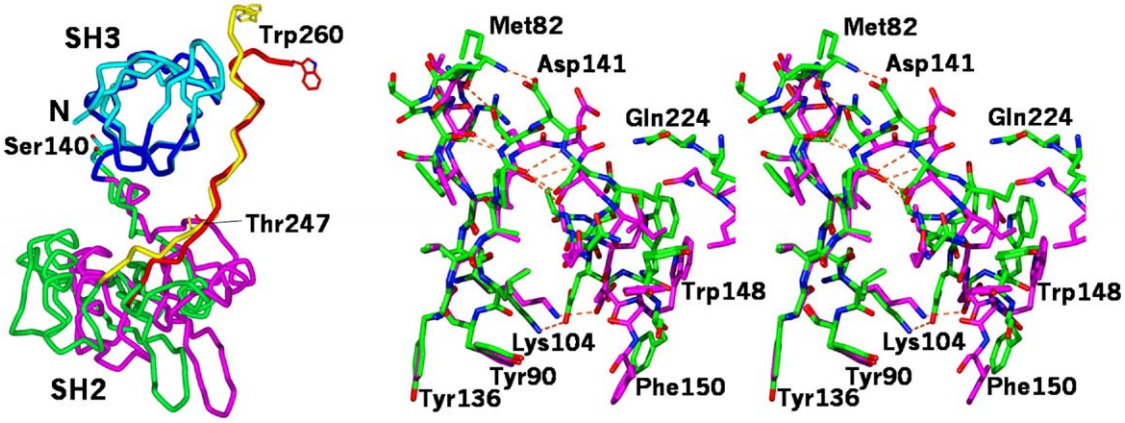

Figure 4. SH3-SH2 Structure

(Left) Superposition of the SH3 and SH2 domains and the linkers from the assembled inactive (dark-blue, red, and magenta) and the unphosphorylated (cyan, green, and yellow) structures, respectively. The superposition is based on residues from the SH3 domain only (84–142) and is viewed from the same orientation as in Figure 2 in order to show how the clamp opens up on release from pTyr527.

(Right) Stereo view of the connector region showing important hydrogen bonds (orange) for unphosphorylated c-Src (green) and pTyr527 c-Src (magenta).

residue Met82, which is not seen in the phosphorylated structures (Xu et al., 1997, 1999).

The binding sites of both of the SH domains are occupied in this structure. That of the SH3 domain is occupied by the linker as in the autoinhibited structure, and the phosphotyrosine binding site of the SH2 domain is occupied by a sulfate ion, that arises from the crystallization buffer. This sulfate lies in a very similar position to the phosphate of other SH2-phosphotyrosine complexes, but in quite a different position to the phosphate of the assembled inactive structure of c-Src (PDB entry 2SRC), which reflects the poor binding of the C-terminal tail of c-Src in the latter structure. In the structure of assembled inactive Hck (Schindler et al., 1999), where the C-terminal tail has been modified to resemble a high-affinity SH2 ligand, the phosphate superimposes well with the sulfate observed here. The rest of the binding site, which is not significantly different as there are only slight shifts in the positions of side chains Arg155, Arg156, Glu178, and Lys203, is occupied by water molecules, and there are also two more sulfate ions in the vicinity.

The SH2-Kinase Linker

The structure of the linker region is also similar to that of the inactive conformation (Figure 4). It superimposes well for the region 245–248 when the SH2 domains are used for the alignment and for the region 250–254 using the SH3 domains are used for alignment. Residues 247–249, where the linker kinks to allow opening of the angle between the two domains, are also the ones that have the highest B values in the linker. The end of the linker beyond the SH3 binding site adopts a different conformation starting from Ala256. Actually, the backbone carbonyl of Leu255 is flipped by 180° so that the linker region can continue in an extended conformation up to Ala259, where residues 258–261 form a β turn that allows Tyr260 to pack against Lys315 from helix αC. This conformation is stabilized in the unphosphorylated c-Src structure by hydrogen bonds between Asp258 and Lys315, the backbone NHs of Trp260 and Glu97, and via a water molecule to Glu261. Further stabilization comes from the hydrogen bond between Glu97 and Trp260. In the monophsophorylated structure, Asp258 faces the solvent.

Conformational Changes in the Kinase Domain

A comparison of the structure of unphosphorylated c-Src with that of the closely related Lck kinase domain in the activated state (Yamaguchi and Hendrickson, 1996) (Figure 5), shows that it adopts an active conformation. Although the Lck structure is of an isolated kinase domain, the orientation of the Lck N terminus superimposes well with the end of the SH2-kinase linker of unphosphorylated c-Src reported here, but it is quite different from the orientation in the assembled inactive state of c-Src. This suggests that the orientation of the SH3 and SH2 domains relative to the kinase domain is determined by the few residues, including Trp260 and Glu261, at the end of the linker region.

The conformation of the activation loop in unphosphorylated c-Src is extended, similar to the conformation of this loop in other active kinases, although it does not adopt the same conformation as it probably would in the phosphorylated state (Figure 5). Phosphorylation of Tyr394 in Lck allows the loop to adopt a conformation suitable for the binding of substrate. This conformation is stabilized by Arg387 (409 in c-Src), Arg363 (385), Ala396 (418) and, possibly, Arg397 (419), all of which coordinate and/or stack against the phosphorylated tyrosine. In the unphosphorylated c-Src structure presented here, the N-terminal part of the activation loop superimposes very well with that of activated Lck (rmsd. of 8 Cα atoms is 0.21 Å). This region, along with helix αEF and the αEF-αF loop, form the surface against which the remainder of the activation loop (411–424) folds. Arg409 forms a cation-aromatic interaction with the unphosphorylated Tyr416, and would shift to make

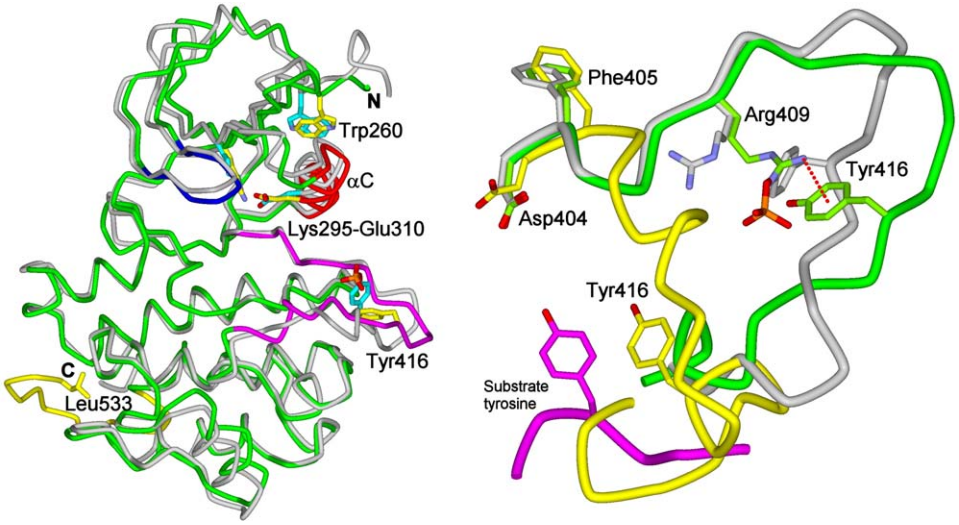

Figure 5. Active Kinase Conformations

(Left) Superposition of activated Lck (gray) and unphosphorylated c-Src (green). The activation loop, the αC helix, the glycine-rich loop and the C-terminal tail of c-Src are colored magenta, red, blue, and yellow, respectively. The Trp260, Lys295, Glu310 and Leu533 side chains are also shown in yellow (c-Src) and cyan (Lck, PDB entry 1QPC). Trp260 of c-Src has the same conformation as in the Lck staurosporine complex (PDB entry 1QPJ, not shown).

(Right) Superpostion of the activation loops of unphosphorylated c-Src (green), pTyr527 c-Src (yellow), and activated Lck (gray). The substrate as bound to activated Irk (magenta) is also shown.

room for the phosphorylated side chain. Tyr416 also has van der Waals interactions with Ala418 and a close contact between the hydroxyl oxygen and Arg385-NH1 (3.2 Å), but no other stabilizing interactions, which is reflected in the relatively high B values of this part of the activation loop. Presumably, the gain of activity on phosphorylation of c-Src Tyr416, as observed for other kinases (Russo et al., 1996), is due to reconstitution of the substrate binding site, as well as stabilization of the conformation of catalytic residues in the active site.

The locations of the catalytic residues of c-Src in the unphosphorylated state are also very similar to those of activated insulin receptor kinase (Irk) in complex with AMP-PNP (Hubbard, 1997). The structural features required for activity are therefore conserved, even though the activation loop of c-Src is not phosphorylated. In addition to the catalytic residues (such as Asp386 and Asn391), the DFG motif (residues 404–406), and the salt bridge (Lys295–Glu310) all superimpose with the equivalent residues in activated Lck and activated Irk. In the monophosphorylated, autoinhibited c-Src structure, the positions of all of these residues are incompatible with activity (Xu et al., 1999).

The C-Terminal Tail and Myristate Binding

The C-terminal leucine binds in a pocket lined with residues from the turn between αD and αE, the end of helix αF and the start of helix αH (Figures 2 and 3). The carboxy terminus has hydrogen bond interactions with the backbone nitrogens of Leu360 and Gly530, and the hydroxyl group of Tyr527. The latter interaction is stabilized by the stacking of Tyr527 against Pro529, which is conserved in all members of the Src family kinases except Hck, Lyn, and Blk (Figure 3). This interaction effectively shields the tyrosine from phosphorylation, which would lead to inactivation of the kinase. The C-terminal tail is shorter for Hck, Lyn, Lck, and Blk, and Pro529 is not strictly conserved in these kinases. If this interaction occurs in Lck, it would not have been seen in the structures because the protein used for crystallization is truncated at the C terminus (Yamaguchi and Hendrickson, 1996).

The myristate binding site is used as a "lock" in the assembled inactive conformation of c-Abl (Nagar et al., 2003) (terminology from Harrison, 2003). Because all of the Src family kinases require myristylation at the N terminus for membrane association and biological activity (Resh, 1994), it is possible that this pocket could also serve as a myristate binding site when Tyr527 is phosphorylated. A comparison of the Abl and c-Src pockets shows that the sequence homology is high and the required conformational changes are slight (Figure 3). At the bottom of the pocket, the increase in size of the c-Src side chain Leu491 compared to Abl Val487 is compensated by a decrease in size of the opposing residue in c-Src (Val364) compared to Abl (Leu360). In the middle of the pocket, c-Src Leu360 is larger than Abl Ala356, but in the absence of the C-terminal tail, there is ample room for the Leu side chain to rotate and leave the pocket open. When comparing the monophosphorylated and unphosphorylated c-Src structures, at the mouth of the pocket, the observed shift of the end of the loop connecting helix αG and helix αH (up to 0.8 Å), with similar magnitudes in the loop between helices αD and αE, shows that there is flexibility to allow for the binding of other ligands.

NMR experiments with unphosphorylated c-Src in the presence of myristate clearly showed no interaction

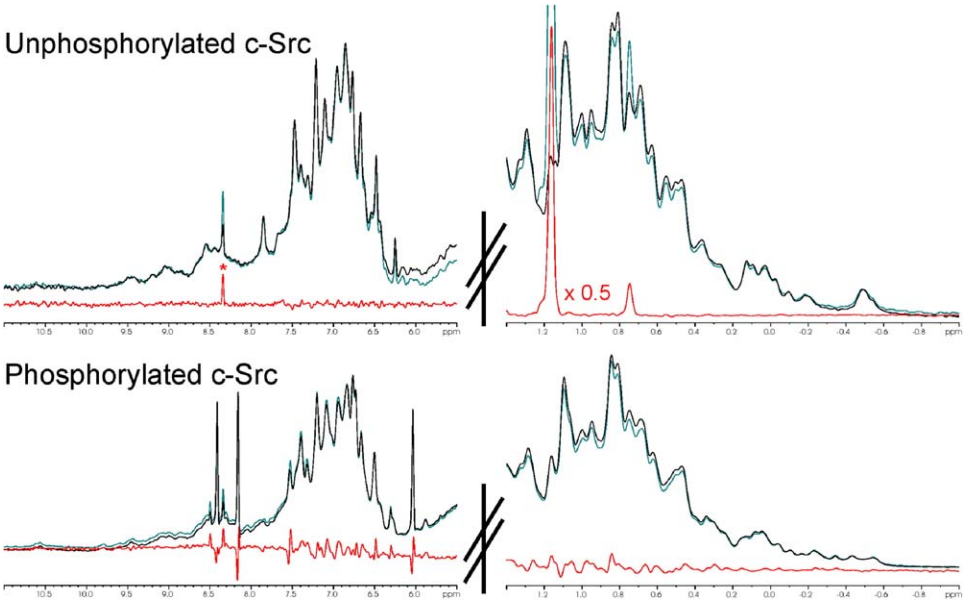

Figure 6. NMR Spectra for Unphosphorylated and Phosphorylated c-Src in Complex with Compound **2**

NMR spectra for unphosphorylated and phosphorylated c-Src in complex with compound **2**, in the presence (blue) and absence (black) of myristate.

(Top panel) The difference spectrum (red) shows sharp myristate signals in the presence of unphosphorylated c-Src, indicating that myristate is tumbling independently and is not interacting with the protein.

(Bottom panel) In the case of phosphorylated c-Src, however, the difference spectrum shows peaks due to chemical shift changes of the protein. In addition, the signals for the fatty acid have become invisible, indicating that myristate interacts with c-Src and thus adopts the broad lines of the protein.

of this fatty acid with the protein (Figure 6). However, after incubation of c-Src with ATP in the presence of C-terminal Src kinase, which is known to phosphorylate Tyr527 (Okada and Nakagawa, 1989), a phosphorylated form of c-Src was obtained that displayed clear spectral differences in the presence and absence of myristate, indicating myristate binding to the protein (Figure 6). Although these results do not indicate the site of binding, the fact that myristate binding is only observed with the phosphorylated protein is consistent with the idea that the Leu533 binding site would be liberated by phosphorylation of Tyr527.

Discussion

Comparison of STI571 and Compound 2 Binding Modes to c-Src and Abl

STI571 stabilizes an autoinhibited state of Abl kinase, requiring the shift of the absolutely conserved DFG motif at the N terminus of the activation loop to bind. The structure reported here shows that the binding mode of compound **2** to c-Src is quite different from that of STI571 bound to Abl (Figure 1), but it is similar to the observed binding mode of STI571 to Syk (Atwell et al., 2004). The coplanar conformation of the pyridinyl, pyrimidinyl, and diaminophenyl groups is less favorable for STI571 due to steric clashes involving the methyl substituent of the diaminophenyl group. However, there is no obvious structural reason why STI571 and **2** cannot bind to c-Src with the STI571 binding mode. From this we can speculate that c-Src is not able to adopt the same autoinhibited conformation that is stabilized in Abl kinase by the binding of STI571. The structures of assembled inactive c-Src and Abl (containing SH3, SH2, and kinase domains) (Xu et al., 1999; Nagar et al., 2003), and the isolated Abl kinase domain (Nagar et al., 2002; Cowan-Jacob et al., 2004), show distinct inactive conformations, supporting this speculation. The conformation of the DFG motif in the assembled inactive Abl structure is different from both the conformation required for activity and that stabilized by the binding of STI571, whereas the rest of the kinase domain adopts an active conformation. STI571 cannot bind to this assembled inactive state without inducing conformational changes, which is reflected in the observed affinity of 400 nM compared to 150 nM for the inactive kinase domain (Hantschel et al., 2003). Neither of these conformations has been observed for the c-Src kinase domain. The elements of kinase sequences that contribute to this restriction have yet to be identified.

Regulation and Activation of c-Src

The structure of cSrc reported here shows an active conformation of the kinase domain despite the lack of phosphorylation of Tyr416 in the activation loop. In cells c-Src is found to be phosphorylated either on Tyr416 (active) or on Tyr527 (inactive), and the unphosphorylated state has not been observed. It is therefore possible that this conformational state has little relevance to what occurs within the cell, and that it may even be induced or stabilized by the presence of the inhibitor. We have also obtained crystal structures of c-Src in the

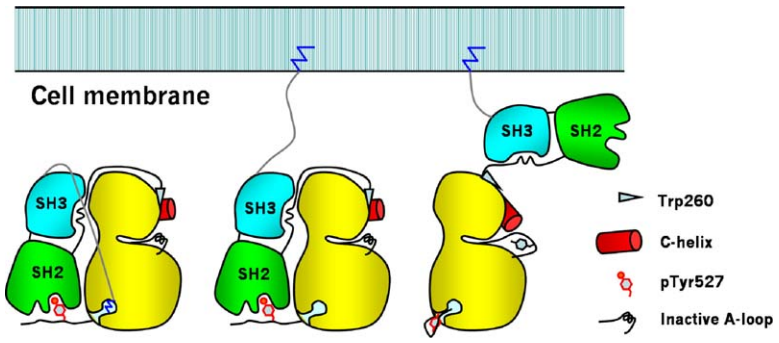

Figure 7. Schematic Diagram Showing a Speculative Model for the Possible Initial Steps in the Activation of c-Src Kinase Based on the Structure of the Unphosphorylated Form and NMR Binding Studies

(Left) The assembled inactive state of c-Src may involve myristate binding to the C-terminal lobe of the kinase (yellow).

(Middle) Myristate binding to the membrane could be the first step in the activation of the kinase.

(Right) Unlatching of the SH2 domain and opening up of the structure makes Tyr416 more accessible for phosphorylation. This is the state observed in the crystal structure reported here.

apo form, with the ATP mimic, AMP-PNP, bound and with other inhibitors (G. Rummel and S.W.C.-J., unpublished data), suggesting that it is not dependent on the type of ligand bound and that it is compatible with the binding of the natural cofactor. The conformation may of course be stabilized by crystal contacts, but would have to exist in solution in order for the crystals to form.

This c-Src structure shows similarities to that of Cdk2. Upon binding of cyclin, the αC helix of Cdk2 swings back into the active site, the residues required for catalysis adopt an active conformation, and subsequent phosphorylation gives full activity (Jeffrey et al., 1995; Russo et al., 1996). The SH3 domain seems to perform a similar action in c-Src. However, the relative orientations of helix αC and the SH3 domain are also favored by the repositioning of Trp260 and surrounding residues. The activation of c-Src observed when the SH3 domain is displaced from the linker by binding to an SH3 ligand (Moarefi et al., 1997; Lerner and Smithgall, 2002) suggests that the presence of the SH3 domain next to helix αC is not necessary for the active conformation. The role of the C-terminal end of the linker in the assembled inactive state may be to pin Trp260 between helix αC and the N lobe β sheet, where it keeps the helix in the inactive or "out" position. Unpinning would occur with the release of the SH3-SH2-linker clamp, so that Trp260 would be free to adopt the conformation observed both here and in the isolated kinase domain of the activated Lck structure (Yamaguchi and Hendrickson, 1996), where it and Glu261 lie at the surface of the protein and do not have a direct influence on the positions of secondary structure elements in the kinase domain. The fact that mutation of Trp260 to alanine has been shown to activate Hck (LaFevre-Bernt et al., 1998), supports this theory.

The structure of unphosphorylated c-Src lends evidence to the "snap-lock" mechanism of kinase autoinhibition (Young et al., 2001), where residues in the SH3-SH2 connector adopt a rigid structure when the two domains are bound to their internal docking sites. This rigidity impedes the activating transition of the kinase. Release of the SH2 domain from pTyr527 leaves the SH3 domain-linker interaction intact, but the structure shows that there is flexibility between the two domains, which also involves the linker. Solution and modeling studies have also shown that the flexibility of the SH3-SH2 connector increases when the two domains are released from the assembled inactive state (Young et al., 2001; Ulmer et al., 2002), and mutation of residues in the connector to glycine leads to constitutative activation of c-Src (Young et al., 2001). All of these findings suggest that any event that results in release of the snap-lock will lead to activation of the kinase. Known activation mechanisms of Src-family kinases (dephosphorylation of the tail, displacement of the tail from the SH2 domain, SH3 domain displacement, mutations in the SH3-SH2 connector, mutations in the SH2-kinase linker, and binding of the kinase N lobe to other proteins) would be expected to cause conformational changes that destabilize the SH3-SH2 linker, therefore allowing Tyr416 to be more accessible for phosphorylation and thus full activation of the kinase. Any event that prevents the snap-lock falling into place, could shift the equilibrium toward the active conformation. For example, the binding of **2**, which requires a larger cleft than AMP-PNP, or the mutation Thr338Ile observed in the adenine site of oncogenic v-Src (Kato et al., 1986), might both favor an opening of the angle between the N- and C-terminal lobes. This could explain the constitutive activation of the latter.

All of these regulation mechanisms support the idea that the mode of activation predetermines the type of downstream signaling that will occur. This hypothesis was put forward based on studies that showed that Hck could be activated by an SH3-specific ligand without tail-release from the SH2 domain (Lerner and Smithgall, 2002), suggesting that SH3-based activation favors signaling that does not involve the SH2 domain. The crystal structure of the isolated Lck SH domains reveals a conformation in which, due to a change in conformation of residues in the SH3-SH2 interface (Asn120, Ser121) relative to other SH tandem structures, the SH3 domain is flipped away from the relative c-Src position by 140°. This type of flexibility would leave room for interaction with SH3 ligands without affecting the rest of the assembled state, although the latter is likely to be more labile. The c-Src structure presented here shows that in the unphosphorylated state the SH2 domain is available for downstream signaling. In both cases phosphorylation of Tyr416 is required for full activity.

The observation that the C-terminal tail is found to bind in a pocket equivalent to the Abl myristate site (Nagar et al., 2003) suggests that Src-family kinases

could also be regulated by myristate binding. We have shown that myristate binds to phosphorylated c-Src, but not to the unphosphorylated form, which could be explained by the blocking of the binding site by Leu533 in the latter case. In cells, if the N-terminal myristate was bound in this pocket, the C-terminal Leu533would be displaced, and Tyr527 would be exposed for phosphorylation, thereby favoring the adoption of the assembled inactive state (Figure 7). Binding of the myristyl group to the membrane would therefore be necessary for activation, as has been observed previously (Resh, 1994). Experimental evidence needs to be obtained to show whether myristate binding to the kinase domain of c-Src actually has a role in regulation and also to confirm the site of myristate binding. To this end, residues in the C-terminal tail binding pocket could be mutated, which would allow experiments to determine if tail binding really protects Tyr527 from phosphorylation in the wild-type protein compared to the mutant. In addition, NMR spectroscopy could be employed to see if the binding of myristate is abolished. Cocrystallization of myristate with pTyr527 c-Src would also be a possibility to confirm the binding site.

c-Src is necessarily a tightly regulated protein due to its ubiquitous distribution and the fact that deregulation leads to oncogenic behavior because of changes in cell growth control, gene expression, metabolism, and cytoskeletal architecture; an extra form of regulation would not be unjustified. One can also speculate that other members of the Src family of kinases could be regulated by myristate binding, because, although the homology of the N-terminal unique region is low, the length of this region is very similar to that of Abl kinase and they are all N-terminally myristoylated or palmitoylated. Although the slightly shorter C terminus of the Hck, Lck, Lyn, and Blk kinases means that the C-terminal tail would not be able to bind to the potential myristate binding pocket in the same way as for c-Src kinase, the residues lining the pocket share high homology (Figure 3).

Experimental Procedures

Preparation of Compound 2

4-[(4-Methyl-1-piperazinyl)methyl]-N-[3-[[4-(3-pyridinyl)-2-pyrimidinyl]amino]phenyl]-benzamide was prepared by 1,3-addition of (3-nitrophenyl)guanidine to 3-(dimethylamino)-1-(3-pyridinyl)-2-propen-1-one, followed by Pd-catalyzed hydrogenation and amidation of the resulting aniline with 4-[(4-methyl-1-piperazinyl)methyl]benzoic acid (Sairam et al., 2003). The product was purified by column chromatography (silica gel; eluent NH_3 (25% aq.)-MeOH-CH_2Cl_2 (1:9:90) followed by recrystallization from EtOAc; melting point, 204°C–208°C).

Preparation of the ATP-Sepharose Column

Adenosine-5′-(γ-4-aminophenyl) triphosphate was synthesized according to a published procedure (Haystead et al., 1993). A total of 0.5 g of the ATP derivative was coupled to 6 g CNBr-activated Sepharose 4B without spacer atoms (Amersham Biosciences) in 0.1 M $NaHCO_3$ buffer for 1.5 hr at room temperature according to the manufacturer's instructions.

Protein Expression and Purification for Structural Studies

A recombinant baculovirus carrying the gene for a deletional mutant of human c-Src (M/ΔG1-G84/V85-L535, human numbering) was kindly provided by M. Eck (Dana-Farber Cancer Institute). Expression in Sf9 cells was carried out in an 8 liter bioreactor (FairMenTec GmbH, Germany) in Excell 400 medium + 5% FCS at 28°C. 200 ml of recombinant baculovirus was added to the culture along with a c-Src inhibitor in 500 ml of TC100 medium with 10% FCS, to give a final inhibitor concentration of 5 μM. After 72 hr, cells were harvested by centrifugation and the pellet was stored at −70°C.

The cell pellet was lysed by sonication in buffer A (20 mM Tris, 5 vol % glycerol, 3 mM DTT [pH 8]) supplemented with additional 2 mM DTT and a protease inhibitor cocktail (Complete, Roche) and the lysate clarified by centrifugation at 45,000 × g. The supernatant was adjusted to pH 8.4 and applied in two portions to a 55 ml column of Source 30 Q equipped with a 15 ml precolumn of SP-sepharose FF. After a wash with buffer A, the precolumn was disconnected and c-Src eluted with a gradient to 200 mM NaCl. After addition of 1 mM EDTA, c-Src-containing fractions were concentrated, NaCl and $MgCl_2$ were added to 300 and 10 mM final concentrations, respectively, and the solution was applied to a 20 ml column of ATP-Sepharose equilibrated with 0.3 M NaCl and 10 mM $MgCl_2$ in buffer B (20 mM HEPES, 5 vol % glycerol, 3 mM DTT, [pH 7.6]). After washing with equilibration buffer, c-Src was eluted with 0.9 M NaCl in buffer B, diluted with an equal volume of buffer B, concentrated, and passed over two HiPrep 26/10 desalting columns connected in series and equilibrated with 120 mM NaCl, 1 mM EDTA in buffer A. Unphoshorylated and monophosphorylated c-Src were separated on a Mono Q HR10/10 column with a gradient from 40 to 280 mM NaCl in buffer A. Unphoshorylated c-Src was applied to a HiLoad 16/60 Superdex 200 column and eluted with 20 mM HEPES, 0.2 M NaCl, 0.2 mM EDTA, 3 mM DTT (pH 7.8). Compound **2** (10 mM in DMSO) was added to a 3-fold molar excess, DTT was increased to 5 mM, and c-Src was concentrated to 15 mg/ml. The concentrated protein was either used immediately for crystallization or aliquoted and stored at −80°C. All purification steps were performed at 4°C and were analyzed by HPLC and SDS-PAGE. Columns and resins used for chromatography were obtained from Amersham Biosciences. c-Src was characterized by LC-MS and N-terminal sequence analysis. Seventy percent of the isolated c-Src was unphosphorylated, 30% was monophosphorylated, and about 15% of both forms had no N-terminal Met residue. The final yield of purified unphosphorylated c-Src was 21 mg. The molar ratio of compound **2** to c-Src was calculated from the HPLC peak areas.

Crystallization and Data Collection

Crystallization screens were performed in 96-well sitting drop plates (Corning): 0.8 μl of protein at 15 mg/ml in 20 mM HEPES, 200 mM NaCl, 0.2 mM EDTA (pH 7.8 with 5 mM DTT) was mixed with 1.0 μl of screening solution and equilibrated with 100 μl of the screening solution. The protein solution contained a 1:1 molar ratio of unphosphorylated c-Src and compound **2**. Optimization was performed in 24-well hanging drop vapor diffusion trays at room temperature. For data collection, crystals grown with 1.3 M ammonium sulfate, 0.1 M Tris (pH 8.0), and 12% glycerol were transferred to the same buffer containing 25% glycerol before direct cooling in the cryo-stream (Oxford Cryosystems Ltd, Oxford, UK) at 100 K. The raw diffraction data were processed with Denzo and Scalepack (HKL Research Inc., Charlottesville, VA).

Structure Determination and Analysis

The structure was determined using tools in the CCP4 graphical user interface (CCP4, 1994) with the automated molecular replacement script MOLREP (Vagin and Teplyakov, 1997). Rigid body refinement of the initial solution was performed with REFMAC5 (Murshudov et al., 1997), before automatic refinement with all of the data using ARP/wARP (Perrakis et al., 1997). Improvement of the model then proceeded with cycles of model building on a Silicon Graphics Inc. Octane with the program O (Jones et al., 1991) and maximum likelihood refinement with REFMAC5. Individual temperature factors were refined, and a bulk solvent correction was used in scaling. Water molecules were added in the latter cycles of refinement using ARP/wARP. Structure comparisons were performed using the program O, analysis of the quality of the model with PROCHECK (Laskowski et al., 1993), and preparation of the images with Molscript (Kraulis, 1991), O, and Molray (Harris and Jones, 2001) or WebLab viewer Lite (Accelrys Inc. USA).

Preparation of Phosphorylated c-Src Kinase for NMR Spectroscopic Measurements

Unphosphorylated cSrc purified for crystallography, as described, and complexed with compound **2** was exchanged into 20 mM Tris-D11, 200 mM NaCl, 0.3 mM EDTA-D12, 3 mM DTT-D10 (pH 7.6). 2 mg c-Src in 1.5 ml of the deuterated buffer was phosphorylated by addition of 5 mM $MgCl_2$, 0.16 mM ATP, and 40 μl CSK at 4°C for 14 hr. The reaction was concentrated to 100 μM c-Src and used without further purification. Analysis by LC-MS showed that 67% of c-Src was monophosphorylated, 12% diphosphorylated, and 21% unphosphorylated. C-terminal c-Src kinase (CSK) from rat spleen was a kind gift of Prof. L.A. Pinna, University of Padova, Italy.

NMR Spectroscopy of Unphosphorylated and Phosphorylated c-Src

NMR spectroscopy was used to probe binding affinity to c-Src of long-chain fatty acids, such as myristate or palmitate. All NMR experiments were recorded at 296 K on a Bruker DRX600 instrument. The c-Src concentration was 100 μmol/l for each experiment, and myristate was present at 100 μmol/l for the blue spectra in Figure 6. In the case of unphosphorylated c-Src, experiments with 500 μmol/l myristate or 500 μmol/l palmitate were also carried out and did not yield chemical shift changes either. All spectra were analyzed using XWinNMR.

Supplemental Data

Supplemental data, including an additional figure, are available at http://www.structure.org/cgi/content/full/13/6/861/DC1/.

Acknowledgments

Data collection for this work was performed at Beamline PX06SA of the Swiss Light Source, Paul Scherrer Institute, Villigen, Switzerland. The authors thank M. Eck (Dana-Farber Cancer Institute) for providing virus for the production of c-Src, and G. Rummel, P. Rheinberger, C. Zwingelstein, P. Graff, and M. Centeleghe for technical support. All authors are employed by Novartis Pharma. A.C., Basel, Switzerland.

Received: December 3, 2004
Revised: March 14, 2005
Accepted: March 14, 2005
Published: June 7, 2005

References

Atwell, S., Adams, J.M., Badger, J., Buchanan, M.D., Feil, I.K., Ingeborg, K., Froning, K.J., Gao, X., Hendle, J., Keegan, K., et al. (2004). A novel mode of gleevec binding is revealed by the structure of spleen tyrosine kinase. J Biol Chem. *279*, 55827–55832.

Boggon, T.J., and Eck, M.J. (2004). Structure and regulation of Src family kinases. Oncogene *23*, 7918–7927.

Capdeville, R., Buchdunger, E., Zimmermann, J., and Matter, A. (2002). Glivec (STI571, imatinib), a rationally developed, targeted anticancer drug. Nat. Rev. Drug Discov. *1*, 493–502.

CCP4 (Collaborative Computational Project, Number 4) (1994). The CCP4 suite: programs for protein crystallography. Acta Crystallogr. D Biol. Crystallogr. *50*, 760–763.

Cowan-Jacob, S.W., Guez, V., Fendrich, G., Griffin, J.D., Fabbro, D., Furet, P., Liebetanz, J., Mestan, J., and Manley, P.W. (2004). Imatinib (STI571) resistance in chronic myelogenous leukemia: molecular basis of the underlying mechanisms and potential strategies for treatment. Mini Rev. Med. Chem. *4*, 285–299.

Deininger, M.W.N., Goldman, J.M., and Melo, J.V. (2000). The molecular biology of chronic myeloid leukemia. Blood *96*, 3343–3356.

Ellis, B. (1994). Purification and characterization of deletional mutations of pp60c-src tyrosine kinase. J. Cell. Biochem. *18B*, 276.

Faderl, S., Talpaz, M., Estrov, Z., and Kantarjian, H.M. (1999). Chronic myelogenous leukemia: biology and therapy. Ann. Intern. Med. *131*, 207–219.

Feng, S., Chen, J.K., Yu, H., Simon, J.A., and Schreiber, S.L. (1994). Two binding orientations for peptides to the Src SH3 domain: development of a general model for SH3-ligand interactions. Science *266*, 1241–1247.

Gorre, M.E., Mohammed, M., Ellwood, K., Hsu, N., Paquette, R., Rao, P.N., and Sawyers, C.L. (2001). Clinical resistance to STI-571 cancer therapy caused by BCR-ABL gene mutation or amplification. Science *293*, 876–880.

Hantschel, O., Nagar, B., Guettler, S., Kretzschmar, J., Dorey, K., Kuriyan, J., and Superti-Furga, G. (2003). A myristoyl/phosphotyrosine switch regulates c-Abl. Cell *112*, 845–857.

Harris, M., and Jones, T.A. (2001). Molray: a web interface between O and the POV-Ray ray tracer. Acta Crystallogr. D Biol. Crystallogr. *57*, 1201–1203.

Harrison, S.C. (2003). Variation on an Src-like theme. Cell *112*, 737–740.

Haystead, C.M., Gregory, P., Sturgill, T.W., and Haystead, T.A. (1993). Gamma-phosphate-linked ATP-sepharose for the affinity purification of protein kinases: rapid purification to homogeneity of skeletal muscle mitogen-activated protein kinase kinase.. Eur. J. Biochem. *214*, 459–467.

Hochhaus, A., and La Rosee, P. (2004). Imatinib therapy in chronic myelogenous leukemia: strategies to avoid and overcome resistance. Leukemia *18*, 1321–1331.

Hubbard, S.R. (1997). Crystal structure of the activated insulin receptor tyrosine kinase in complex with peptide substrate and ATP analog. EMBO J. *16*, 5572–5581.

Hughes, T.P., Kaeda, J., Branford, S., Rudzki, Z., Hochhaus, A., Hensley, M.L., Gathmann, I., Bolton, A.E., van Hoomissen, I.C., Goldman, J.M., et al. (2003). Frequency of major molecular responses to imatinib or interferon alfa plus cytarabine in newly diagnosed chronic myeloid leukemia. N. Engl. J. Med. *349*, 1423–1432.

Jeffrey, P.D., Russo, A.A., Polyak, K., Gibbs, E., Hurwitz, J., Massague, J., and Pavletich, N.P. (1995). Mechanism of CDK activation revealed by the structure of a cyclin A-CDK2 complex. Nature *376*, 313–320.

Jones, T.A., Zou, J.Y., Cowan, S.W., and Kjeldgaard, M. (1991). Improved methods for building protein models in electron density maps and the location of errors in these models. Acta Crystallogr. A *47*, 110–119.

Kantarjian, H.M., Cortes, J., O'Brien, S., Giles, F.J., Albitar, M., Rios, M.B., Shan, J., Faderl, S., Garcia-Manero, G., Thomas, D.A., et al. (2002). Imatinib mesylate (STI571) therapy for Philadelphia chromosome-positive chronic myelogenous leukemia in blast phase. Blood *99*, 3547–3553.

Kato, J., Takeya, T., Grandori, C., Iba, H., Levy, J.B., and Hanafusa, H. (1986). Amino acid substitutions sufficient to convert the nontransforming p60c-src protein to a transforming protein. Mol. Cell. Biol. *6*, 4155–4160.

Kraulis, P.J. (1991). MOLSCRIPT: a program to produce both detailed and schematic plots of protein structures. J. Appl. Crystallogr. *24*, 945–949.

LaFevre-Bernt, M., Sicheri, F., Pico, A., Porter, M., Kuriyan, J., and Miller, W.T. (1998). Intramolecular regulatory interactions in the Src family kinase Hck probed by mutagenesis of a conserved tryptophan residue. J. Biol. Chem. *273*, 32129–32134.

Laskowski, R.A., MacArthur, M.W., Moss, D.S., and Thornton, J.M. (1993). PROCHECK: a program to check the stereochemical quality of protein structures. J. Appl. Crystallogr. *26*, 283–291.

Lerner, E.C., and Smithgall, T.E. (2002). SH3-dependent stimulation of Src-family kinase autophosphorylation without tail release from the SH2 domain in vivo. Nat. Struct. Biol. *9*, 365–369.

Moarefi, I., LeFevre-Bernt, M., Sicheri, F., Huse, M., Lee, C.H., Kuriyan, J., and Miller, W.T. (1997). Activation of the Src-family tyrosine kinase Hck by SH3 domain displacement. Nature *385*, 650–653.

Murshudov, G.N., Vagin, A.A., and Dodson, E.J. (1997). Refinement of macromolecular structures by the maximum-likelihood method. Acta Crystallogr. D Biol. Crystallogr. *53*, 240–255.

Nagar, B., Bornmann, W.G., Pellicena, P., Schindler, T., Veach, D.R.,

Miller, W.T., Clarkson, B., and Kuriyan, J. (2002). Crystal structures of the kinase domain of c-Abl in complex with the small molecule inhibitors PD173955 and imatinib (STI-571). Cancer Res. *62*, 4236–4243.

Nagar, B., Hantschel, O., Young, M.A., Scheffzek, K., Veach, D., Bornmann, W., Clarkson, B., Superti-Furga, G., and Kuriyan, J. (2003). Structural basis for the autoinhibition of c-Abl tyrosine kinase. Cell *112*, 859–871.

O'hare, T., Pollock, R., Stoffregen, E.P., Keats, J.A., Abdullah, O.M., Moseson, E.M., Rivera, V.M., Tang, H., Metcalf, C.A., III, Bohacek, R.S., et al. (2004). Inhibition of wild-type and mutant Bcr-Abl by AP23464, a potent ATP-based oncogenic protein kinase inhibitor: implications for CML. Blood *104*, 2532–2539.

Okada, M., and Nakagawa, H. (1989). A protein tyrosine kinase involved in regulation of pp60c-src function. J. Biol. Chem. *264*, 20886–20893.

Perrakis, A., Sixma, T.K., Wilson, K.S., and Lamzin, V.S. (1997). wARP: improvement and extension of crystallographic phase by weighted averaging of multiple-refined dummy atomic models. Acta Crystallogr. D Biol. Crystallogr. *53*, 448–455.

Pluk, H., Dorey, K., and Superti-Furga, G. (2002). Autoinhibition of c-Abl. Cell *108*, 247–259.

Resh, M.D. (1994). Myristylation and palmitylation of Src family members: the fats of the matter. Cell *76*, 411–413.

Russo, A.A., Jeffrey, P.D., and Pavletich, N.P. (1996). Structural basis of cyclin-dependent kinase activation by phosphorylation. Nat. Struct. Biol. *3*, 696–700.

Sairam, P., Puranik, R., Kelkar, A.S., Sasikiran, S., Veerender, M., and Parvathi, A. (2003). The ester and amide derivatives of 4-(4-Methyl Piperazinomethyl) benzoic acid. Synthetic Communications *33*, 3597–3605.

Sawyers, C.L. (1999). Chronic myeloid leukemia. N. Engl. J. Med. *340*, 1330–1340.

Schindler, T., Bornmann, W., Pellicena, P., Miller, W.T., Clarkson, B., and Kuriyan, J. (2000). Structural mechanism for STI-571 inhibition of Abelson tyrosine kinase. Science *289*, 1938–1942.

Schindler, T., Sicheri, F., Pico, A., Gazit, A., Levitzki, A., and Kuriyan, J. (1999). Crystal structure of Hck in complex with a Src family-selective tyrosine kinase inhibitor. Mol. Cell *3*, 639–648.

Shah, N.P., Tran, C., Lee, F.Y., Chen, P., Norris, D., and Sawyers, C.L. (2004). Overriding imatinib resistance with a novel ABL kinase inhibitor. Science *305*, 399–402.

Sicheri, F., Moarefi, I., and Kuriyan, J. (1997). Crystal structure of the Src family tyrosine kinase Hck. Nature *385*, 602–609.

Ulmer, T.S., Werner, J.M., and Campbell, I.D. (2002). SH3-SH2 domain orientation in Src kinases: NMR studies of Fyn. Structure *10*, 901–911.

Vagin, A., and Teplyakov, A. (1997). MOLREP: an automated program for molecular replacement. J. Appl. Crystallogr. *30*, 1022–1025.

Waksman, G., Kominos, D., Robertson, S.C., Pant, N., Baltimore, D., Birge, R.B., Cowburn, D., Hanafusa, H., and Mayer, B.J. (1992). Crystal structure of the phosphotyrosine recognition domain SH2 of v-src complexed with tyrosine-phosphorylated peptides. Nature *358*, 646–653.

Warmuth, M., Damoiseaux, R., Liu, Y., Fabbro, D., and Gray, N. (2003). Src family kinases: potential targets for the treatment of human cancer and leukemia. Curr. Pharm. Des. *9*, 2043–2059.

Williams, J.C., Weijland, A., Gonfloni, S., Thompson, A., Courtneidge, S.A., Superti-Furga, G., and Wierenga, R.K. (1997). The 2.35 A crystal structure of the inactivated form of chicken Src: a dynamic molecule with multiple regulatory interactions. J. Mol. Biol. *274*, 757–775.

Xu, W., Doshi, A., Lei, M., Eck, M.J., and Harrison, S.C. (1999). Crystal structures of c-Src reveal features of its autoinhibitory mechanism. Mol. Cell *3*, 629–638.

Xu, W., Harrison, S.C., and Eck, M.J. (1997). Three-dimensional structure of the tyrosine kinase c-Src. Nature *385*, 595–602.

Yamaguchi, H., and Hendrickson, W.A. (1996). Structural basis for activation of human lymphocyte kinase Lck upon tyrosine phosphorylation. Nature *384*, 484–489.

Young, M.A., Gonfloni, S., Superti-Furga, G., Roux, B., and Kuriyan, J. (2001). Dynamic coupling between the SH2 and SH3 domains of c-Src and Hck underlies their inactivation by C-terminal tyrosine phosphorylation. Cell *105*, 115–126.